scientific reports

Check for updates

OPEN

Mutational and low-coverage whole genome sequencing identifies actionable DNA repair alterations in prostate cancer plasma DNA

Alessandra Virga[1], Milena Urbini[1]✉, Maurizio Polano[2], Elisabetta Petracci[3], Gianluca Tedaldi[1], Giorgia Gurioli[1], Giorgia Marisi[1], Davide Angeli[3], Andrea Ambrosini-Spaltro[4], Giovanni De Luca[5], Ilaria Cangini[1], Valentina Zampiga[1], Giovanna Cenacchi[6], Giuseppe Toffoli[2], Chiara Casadei[7], Maria Concetta Cursano[8], Vincenza Conteduca[9], Ugo De Giorgi[8,10,11] & Paola Ulivi[1,11]

PARP inhibitors (PARPi), recently introduced for treating metastatic castration-resistant prostate cancer (mCRPC), have heightened interest in molecular profiling for pathogenic aberrations in homologous recombination DNA repair (HRR) genes in all mCRPC patients. Liquid biopsy offers a viable alternative to archival tumor tissue for genetic analysis. In this study, we assessed the feasibility and utility of combining mutational panel sequencing with shallow whole genome sequencing (sWGS) to refine HRR status determination from plasma in prostate cancer (PCa) patients. The mutational profile of 16 HRR genes was assessed in 63 PCa patients: 28.6% of patients harbored putative pathogenic variants in HRR-related genes. A HRR-mutant status was defined for 10 patients (15.8%). Through the integration of sWGS data, plasma samples non-informative about somatic alterations were identified, and germline/somatic origin of HRR mutations was defined. Matched tumor tissue was available for 41 patients, with an 85.7% concordance rate between plasma and tissue mutational analyses. Additionally, we explored the copy number variation (CNV) profile using sWGS and it was found concordant with the literature PCa profiles. Our findings demonstrated that ctDNA analysis through liquid biopsy is a reliable alternative to tissue-based methods for identifying SNVs and CNVs. However, concordance was affected by ctDNA levels in plasma and clonal hematopoiesis. The data highlight the utility of integrating sWGS with targeted mutation analysis for comprehensive molecular profiling of PCa patients.

Keywords Prostate cancer, Liquid biopsy, PARP inhibitors, Low-coverage WGS

Abbreviations

PCa	Prostate cancer.
HRR	Homologous recombination DNA repair.
mCRPC	Metastatic castration-resistant PCa.

[1]Biosciences Laboratory, IRCCS Istituto Romagnolo per lo Studio dei Tumori (IRST) "Dino Amadori", Meldola, Italy. [2]Experimental and Clinical Pharmacology Unit, Centro di Riferimento Oncologico di Aviano, Istituto di Ricovero e Cura a Carattere Scientifico, Aviano, Italy. [3]Unit of Biostatistics and Clinical Trials, IRCCS Istituto Romagnolo per lo Studio dei Tumori (IRST) "Dino Amadori", Meldola, Italy. [4]Pathology Unit, "Morgagni-Pierantoni" Hospital, AUSL Romagna, Forlì, Italy. [5]Pathology Unit, "Maurizio Bufalini" Hospital, Cesena 47521, Italy. [6]Department of Biomedical and Neuromotor Sciences (DIBINEM), University of Bologna, Bologna, Italy. [7]Medical Oncology, Breast & GYN Unit, IRCCS Istituto Romagnolo per lo Studio dei Tumori (IRST) "Dino Amadori", Meldola, Italy. [8]Department of Medical Oncology, IRCCS Istituto Romagnolo per lo Studio dei Tumori (IRST) "Dino Amadori", Meldola, Italy. [9]Department of Medical and Surgical Sciences, Unit of Medical Oncology and Biomolecular Therapy, University of Foggia, Policlinico Riuniti, Foggia, Italy. [10]University Oncology Unit, University of Salento, Fazzi Hospital, Lecce, Italy. [11]Ugo De Giorgi and Paola Ulivi contributed equally to this work. ✉email: milena.urbini@irst.emr.it

PARPi	Poly ADP-ribose polymerase inhibitors.
sWGS	Shallow whole-genome sequencing.
RT	Radiotherapy.
ct	Circulating tumor.
CNV	Copy number variation.
CNVs	Copy number variations.
mPCa	Metastatic PCa.
ADT	Androgen deprivation therapies.
FDA	Food and Drug Administration.
PD	Disease progression.
WBC	White blood cells.
FFPE	Formalin-fixed paraffin-embedded.
TURB	From trans-urethral resection of the bladder.
HRS	Homologous Recombination Solutions™.
HCS	Hereditary Cancer Solution™.
QC	Quality control.
VAF	Variant allele frequency.
VUS	Uncertain significance.
TF	Tumor fraction.
mHSPC	Metastatic hormone-sensitive PCa.
GS	Gleason score.

Prostate cancer (PCa) is the most frequently diagnosed cancer in men, with 268.490 new cases in the United States and 34.500 deaths estimated to occur in 2022[1–3]. While surgical treatment and radiotherapy (RT) are the gold standards for localized disease, approximately 25% of patients experience recurrence, leading to progression to metastatic PCa (mPCa). Additionally, 10% of patients present with metastases at the time of diagnosis[4]. Therapeutic options for mPCa include androgen deprivation therapy (ADT), androgen receptor signaling inhibitors (e.g., abiraterone, enzalutamide, darolutamide), and chemotherapy. Prognostic biomarkers may help to distinguish indolent from aggressive variants and could improve personalized treatment strategies[5–8]. Recent advances in targeted therapies have led to the development and clinical implementation of poly ADP-ribose polymerase inhibitors (PARPi) for metastatic castration-resistant prostate cancer (mCRPC)[9,10]. The U.S. Food and Drug Administration (FDA) has approved olaparib and rucaparib for patients harboring germline or somatic mutations in key homologous recombination repair (HRR) genes. These approvals are based on findings from pivotal clinical trials such as PROfound and TRITON-3, which demonstrated improved outcomes for patients with HRR mutations, particularly in *BRCA1* and *BRCA2* genes[11–13]. Moreover, the combination of PARPi with androgen receptor signaling inhibitors has shown promising results in recent studies, although further research is required to optimize patient selection based on *BRCA* and HRR status[14–16]. The genetic landscape of advanced PCa is complex, characterized by numerous somatic mutations, copy number variations (CNVs), and chromosomal aberrations. The identification of these alterations can guide the use of personalized therapies, particularly in the context of PARPi sensitivity. HRR gene mutations, including those in *BRCA1* and *BRCA2*, have been associated with a shorter time to the development of castration-resistant disease, underscoring the importance of obtaining HRR status at the time of metastatic diagnosis[17–19]. Beyond PARPi, HRR mutations have also been linked to platinum-based chemotherapy responses in late-stage mCRPC and to increased PSMA expression, suggesting broader clinical utility of these biomarkers[20–23]. In addition, in small series of patients with mCRPC treated with Lutetium-PSMA, *BRCA* mutations seemed to predict favourable clinical outcomes[24,25]. While tumor tissue is the most common source for genomic analysis, its utility is often limited by the heterogeneity of prostate cancer and challenges in obtaining high-quality samples from metastatic sites. Many real-world PCa patients lack sufficient tissue for analysis due to factors such as diagnostic depletion, low tumor content, or DNA degradation[26–28]. Liquid biopsy, which includes circulating tumor DNA (ctDNA) in the blood, has emerged as a promising alternative for identifying tumor mutational profiles, offering a less invasive and more accessible method[29–32]. Liquid biopsy is also advantageous for monitoring tumor evolution during treatment, especially in cases where *BRCA1/2* reverse mutations or other resistance mechanisms develop in response to PARPi therapy[33–35]. In this study, we analyzed HRR gene alterations in a cohort of PCa patients, using both tumor tissue and liquid biopsy, to evaluate the feasibility of ctDNA for mutational profiling. In addition to targeted mutational analysis, we performed shallow whole-genome sequencing (sWGS) to improve detection of copy number alterations and estimate tumor fraction release in plasma samples. This combined approach aims to enhance the molecular characterization of PCa and support the clinical use of liquid biopsy in personalized medicine.

Methods

Patient cohort

This prospective study, with protocol code 0004169/2017 approved on 15/06/2017, was authorized by the Institutional Review Board of IRCCS Istituto Romagnolo per lo Studio dei Tumori (IRST) "Dino Amadori," Meldola, Italy. The inclusion criteria were patients with a histologically confirmed diagnosis of PCa, classified as acinar adenocarcinoma without neuroendocrine differentiation, at a local or advanced stage, requiring adequate tumor tissue and sufficient circulating DNA for analysis. All patients who met the current criteria from September 1, 2017, to December 31, 2021 were eligible for inclusion in this retrospective study. Clinical history and follow-up data were collected and merged. The study was conducted in compliance with the Declaration

of Helsinki and the Good Clinical Practice Guidelines of the International Conference on Harmonization, and written informed consent was obtained from all patients.

Study design and sample collection

A peripheral blood sample was collected from 63 patients affected by advanced PCa at the IRST IRCCS. Samples were collected in EDTA-containing tubes at baseline (pretreatment) for 47 patients (75%) and for the other 16 patients (25%) at different time points during treatment: 3 at disease progression (PD) and 13 during treatment. The plasma was isolated and stored at −80 °C until DNA extraction. For a subgroup of 12 patients, white blood cells (WBCs) were isolated and stored at −80 °C until DNA extraction. The matched formalin-fixed paraffin-embedded (FFPE) sample of prostate tumor tissue was available for 41 patients and was retrieved from the Pathology Units of Morgagni Pierantoni Hospital (Forlì) and Bufalini Hospital (Cesena). Tumor tissues were obtained from prostatectomy in 13 patients, from biopsies in 25 patients, and from transurethral resection of the bladder (TURB) in 3 patients. Timing corresponded to the surgical process when available or at different time points if biopsy or TURB was performed. A schematic representation of the analysis performed for each sample, as described above, is shown in Fig. 1, and all the sequencing data are available in the supplementary materials.

DNA isolation and quantification

DNA was extracted from 2 ml of plasma, using the QIAamp Circulating Nucleic Acid Kit (Qiagen, Hilden, Germany) according to the manufacturer's instructions. Total extracted DNA was quantified by the fluorimetric instrument Qubit dsDNA HS kit (Thermo Fisher Scientific, Waltham, MA, USA), using 2 µl of DNA. A dedicated pathologist, who selected the more representative tumor area, evaluated FFPE specimens. Seven 10-µm sections were cut for each prostatectomy, TURB, or biopsy sample. The neoplastic area was scraped to collect tumor-derived DNA. The QIAamp DNA FFPE Tissue Kit (Qiagen) was used for DNA isolation. Genomic DNA was extracted using the QIAamp DNA Mini Kit (Qiagen, Hilden, Germany) according to the manufacturer's instructions and quantified using the Qubit dsDNA BR Assay Kit (Thermo Fisher Scientific, Waltham, MA, USA). WBCs were isolated from peripheral blood biospecimens and stored at − 80 °C. Genomic DNA was extracted from 80 µl of WBCs using the QIAamp DNA Mini Kit (Qiagen, Hilden, Germany) and quantified with Qubit dsDNA BR Assay Kit using a Qubit fluorometer (Thermo Fisher Scientific, Waltham, MA, USA).

Library preparation and sequencing

Libraries were generated using the Homologous Recombination Solutions™ (HRS) kit of SOPHiA GENETICS (Saint Sulpice, Switzerland) for plasma and FFPE samples, covering 15 HRR-related genes, *ATM*, *BARD1*, *BRCA1*, *BRCA2*, *BRIP1*, *CDK12*, *CHEK1*, *CHEK2*, *FANCL*, *PALB2*, *PPP2R2A*, *RAD51B*, *RAD51C*, *RAD51D*, *RAD54L*, and *TP53*.

For FFPE specimens, libraries were generated starting from 50 to 200 ng of DNA according to the manufacturer's instructions. Briefly, DNA was enzymatically fragmented and, after tagmentation, ligated to specific adapters. After amplification, Illumina-compatible DNA libraries were subsequently obtained. Two hundred ng of each DNA library was used for 16-gene panel enrichment following the manufacturer's instructions. For circulating

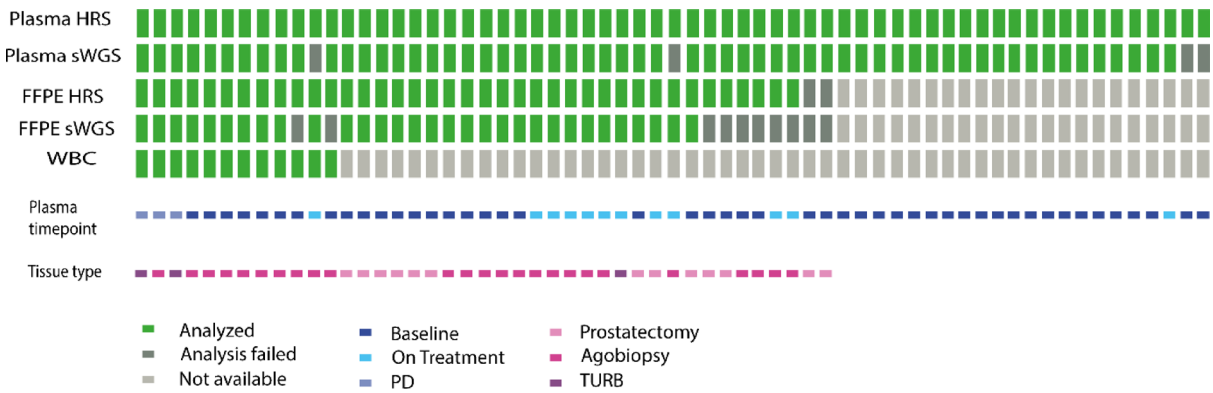

Fig. 1. Biological specimens analyzed in the study. Molecular analysis and characteristics of samples (plasma, tissue and WBC) analyzed in the present paper are shown. Each column represents one patient, and each row represents a different type of analysis. A green box indicates a successful analysis, a dark gray box indicates a failed analysis, and a light gray box indicates an analysis not performed or sample not available for analysis. The HRS target panel was used for the analysis of 63 plasma samples, 59 of which were also evaluated by sWGS analysis. A matched FFPE sample was available for 41 patients, and the HRS panel test was effectively performed in 39 cases. Among the FFPE samples, 31 tissues were analyzed with sWGS. Finally, for a subgroup of 12 patients, the results obtained from tissue and plasma DNA were matched with germline DNA from WBC samples, which were analyzed with the HCS target panel. The lower part of the figure described the plasma time point and tissue type. Abbreviations: PD, progression disease; HRS. Homologous recombination solution; sWGS, shallow whole genome sequencing; FFPE, formalin-fixed, paraffin-embedded; TURB, trans-urethral resection of the bladder.

DNA, 20–70 ng of DNA was used as the starting material, and libraries were generated following the same protocol used for FFPE tissue without fragmentation, according to the manufacturer's instructions. Libraries were then quantified using the Qubit instrument (Thermo Fisher Scientific, Waltham, MA, USA), and quality was evaluated on the Bioanalyzer instrument (Agilent Technologies, USA). After quality and quantity control, the libraries were sequenced on the NextSeq 550 platform, reaching average coverage values of 14855x and 10530x for the plasma and FFPE samples, respectively. We used an aliquot of the same libraries (taken before the enrichment step) to perform sWGS, as described below. Libraries were sequenced on a NextSeq 550 platform with an average coverage of 0.98x for plasma and 0.68x for FFPE.

The germline analysis on WBC was used to determine the germline/somatic status or to exclude clonal hematopoiesis (CH) origin of the alterations detected on the corresponding plasma sample, when necessary. For the germline analysis, libraries were prepared starting from 200 ng of genomic DNA using SOPHiA Hereditary Cancer Solution™ (HCS) v1.1 by SOPHiA GENETICS (Saint Sulpice, Switzerland). The HCS panel included 26 cancer predisposition genes (*ABRAXAS1*, *APC*, *ATM*, *BARD1*, *BRCA1*, *BRCA2*, *BRIP1*, *CDH1*, *CHEK2*, *EPCAM*, *MLH1*, *MRE11*, *MSH2*, *MSH6*, *MUTYH*, *NBN*, *PALB2*, *PIK3CA*, *PMS2*, *PTEN*, *RAD50*, *RAD51C*, *RAD51D*, *STK11*, *TP53* and *XRCC2*). Enriched libraries were sequenced using the MiSeq® Reagent Kit v3 600 cycles (Illumina, San Diego, CA, USA), 2 × 151, on a MiSeq® platform (Illumina, San Diego, CA, USA).

Gene panel variant analysis

Alignment, base calling and variant annotation were performed with SOPHiA DDM® software v4-4.6.2. The fastQ sequences were uploaded after sequencing, and the pipeline for mutational HRS analysis was used for both FFPE DNA and cfDNA analysis. The NGS data were classified after a quality control check based on coverage, depth of sequencing and percentage of mapped reads. Sequences were aligned to the human reference genome hg19 (GRCh37), and an average coverage of 14855x was reached after deduplication. An average of 21,324,320 (98.51%) mapped reads were obtained from plasma sequencing. For the FFPE libraries, an average coverage of 10530x was reached, and an average of 18,283,014 (97.78%) mapped reads were obtained. Variants with a variant allele frequency (VAF) greater than 0.06% were called. Variants frequently present in the normal population (GnomAD > 1%) were excluded[36]. The pathogenicity of the variants was defined following ACMG guidelines (American College of Medical Genetics and Genomics)[37]. Variants classified as "pathogenic" or "likely pathogenic" by VarSome (VarSome Clinical 11.7.5 - https://landing.varsome.com/varsome-clinical) were considered clearly pathogenic and retained in the analysis together with variants of uncertain significance (VUS). Alterations classified as "benign" or "likely benign" by Varsome were excluded[37]. Mutations detected with a VAF > 5% in FFPE tissue or with a VAF > 1% in plasma were retained for analysis. Both germline and somatic alterations were considered in the study, as both are potential targets for PARPi personalized therapy. For the concordance agreement between tissue and plasma, all mutations (pathogenic and VUS) affecting all genes targeted by the HRS panel were considered.

Shallow WGS analysis

The sWGS was performed starting from libraries before the enrichment step. Libraries were sequenced on a NextSeq 550 platform with an average coverage of 0.98x for plasma and 0.68x for FFPE. Shallow WGS data were analyzed using the R-based tool ichorCNA v0.2.0 (https://github.com/broadinstitute/ichorCNA), following standard procedure[38]. Briefly, readCounter function of HMMcopy 1.48.0 suite (https://bioconductor.org/packages/release/bioc/html/HMMcopy.html) was used for generating read count coverage information, then copy number analysis and prediction of tumor fraction (TF) was performed using ichorCNA R package. The TF was estimated for plasma samples, and a cutoff of 0.03 (sensitivity threshold determined by ichorCNA) was set to indicate the presence of ctDNA. FFPE and plasma samples that did not pass quality checks on sWGS analysis (coverage > 0.1x and MAD < 0.150) were excluded from the analysis. For CNV analysis, only autosomal chromosomes were considered. For each sample, the CNV burden was estimated using the total genomic length of CNV alterations identified calculated as a percentage of the size of the autosomal genome. CNV profiles obtained from FFPE and plasma samples were compared with the CNV profile of a publicly available prostate cancer dataset downloaded from cBioPortal (MSK-impact)[39]. To estimate the agreement between CNVs detected by FFPE and matched plasma all segments with CN states different from neutrality were counted and compared between matched samples.

HRR and HRS status definitions

Samples harboring at least one mutation classified as pathogenic or VUS on the gene targeted by the HRS panel, were classified as "HRS-mutant". Conversely, samples with no alteration but with a TF estimate greater than 0.03 were considered as "HRS-wildtype". Samples in which no alterations and no TF was detected were classified as "non-informative".

For the evaluation of HRR mutational status, only the key genes involved in the HRR system (*ATM*, *BARD1*, *BRCA1*, *BRCA2*, *BRIP1*, *CDK12*, *CHEK1*, *CHEK2*, *FANCL*, *PALB2*, *PPP2R2A*, *RAD51B*, *RAD51C*, *RAD51D*, *RAD54L*), and only clear pathogenic mutations (VUS excluded) were considered[11,12]. Samples with mutations fulfilling these requisites were defined as "HRR-mutant".

Statistical analysis

The data were summarized as the mean ± standard deviation (SD) or median, interquartile (IQ) range and the minimum and maximum value, as appropriate, for the continuous variables and through natural frequencies and percentages for the categorical ones. The associations between the categorical variables were tested by Pearson's $\chi 2$ test or Fisher's exact test, as appropriate. To test the agreement between the same determinations

made on two different biological specimens, we applied Cohen's kappa. Conventionally, values ≤ 0.20 indicate poor agreement; values between 0.21 and 0.40 that there is modest agreement; values between 0.41 and 0.60 that there is moderate agreement; values between 0.61 and 0.80 that there is substantial agreement; and values above 0.80 that there is a near-perfect degree of agreement. All analyses were carried out using STATA 15.0 software (College Station, TX).

Results

Patient clinical characteristics

Patient clinical characteristics are shown in Table 1. Overall, 48 (76,2%) of the 63 patients had metastatic disease: 26 (54,2%) patients had metastatic hormone-sensitive PCa (mHSPC), whereas 22 (45,8%) had mCRPC. Fifteen (23,8%) patients had locally advanced PCa, including 11 HSPC patients and 4 CRPC patients. The case series included 22 (36,1%) patients with Gleason score (GS) < 8 and 39 (63,9%) patients with a GS ≥ 8; for 2 patients, the GS was not available.

Detection of alterations on HRR genes from plasma

Plasma samples from 63 patients with a diagnosis of PCa who underwent HRS and sWGS testing by plasma-NGS were included in the cohort (Fig. 1). HRS panel analysis was effective for all patients, and 33 alterations were identified in 18 (28.6%) patients. Mutations (27 classified as pathogenic, 6 VUS) were detected in plasma with a median VAF of 18%, ranging from 1.0 to 61.6%. Among these alterations, 24% were on *TP53*, 10% on *ATM*,

	n	%
Age at liquid biopsy		
Median [IQ - IIIQ]	72.2 [66.3–77.0]	
Min - max	47.3–87.0	
Time point		
Baseline	47	74.6
On treatment	13	20.6
PD	3	4.8
Diagnosis		
Localized disease	11	17.5
CRPC	4	6.4
mCRPC	22	34.9
mHSPC	26	41.3
Metastasis site‡:		
Lymph nodes	26	54.2
Bone	34	70.8
Visceral	3	6.3
Radiotherapy		
No	43	68.3
Yes	20	31.8
Gleason Score		
6	1	1.6
7(3 + 4)	8	13.1
7(4 + 3)	13	21.3
8	20	32.8
9	16	26.2
10	3	4.9
ECOG PS		
0	49	79.0
1	11	17.7
2	2	3.2
Missing	1	

Table 1. Patients' clinical characteristics. ‡Related to mCRPC and mHSCP patients only. IQ: first quartile; IIIQ: third quartile; WT: wild type; PS: performance status. Percentages may not equal 100 due to rounding. Abbreviations: PD, progression disease; CRPC, castration-resistant prostate cancer; mCRPC, metastatic castration-resistant prostate cancer; mHSPC metastatic hormone-sensitive prostate cancer; RT, radiation therapy; ECOG PS, ECOG Performance Status.

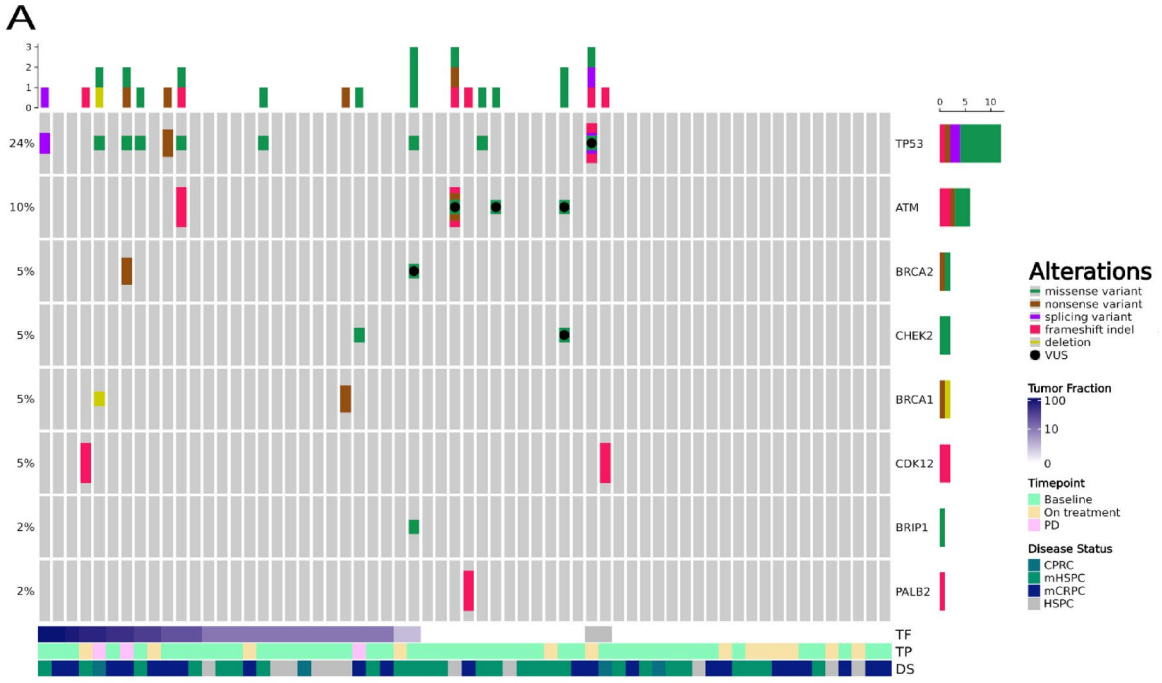

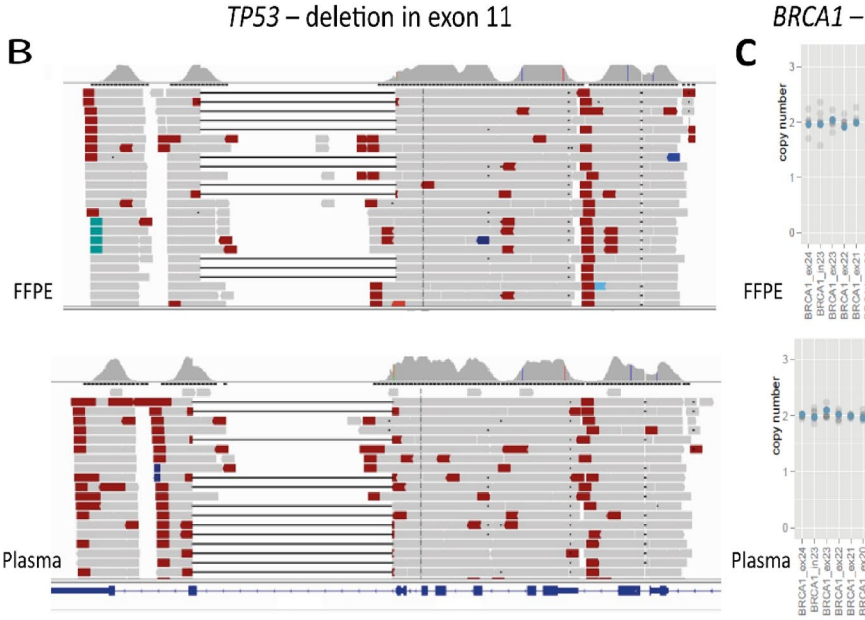

Samples	Gene	Exon	c.DNA	VAF%
0360_FFPE	*TP53*	11	c.*12+42_*70del	19,4
0360_plasma	*TP53*	11	c.*12+42_*70del	26,3

Samples	Gene	Exon	CN
0130_FFPE	*BRCA1*	2-13	1,4
0130_plasma	*BRCA1*	2-13	1,6

5% on both *BRCA2* and *BRCA1* and *CDK12 and CHEK2*, while *BRIP1* and *PALB2* were each mutated in only one patient (2%) (Fig. 2A). Half of the VUS were on *ATM* (Suppl. Table 1). The predominant type of alteration detected was SNVs (66.7%) consisting of 18 missense, 3 nonsense and 1 splicing. Small indels (8 frameshift, 1 splicing) and 1 multi-exonic deletion was found in 33.3% of cases. Interestingly, a novel complex event of 2508 nucleotides (c.*12+42_*70del) affecting *TP53* was identified and a multi-exonic deletion in *BRCA1*, spanning exon 2 to exon 13, were identified (Fig. 2B,C). No significant associations were found between the presence of mutations on genes of the HRS panel and the clinicopathological characteristics of the patients (Suppl. Table 2).

Then, HRR status of each sample was defined considering only the pathogenic alterations covered by the HRS panel with the exception of *TP53*. In total 10 patients (15.8%) were identified as HRR-mutant through the plasma analysis (Suppl. Table 1).

Improvement of HRR mutational call through the combination of sWGS to HRS panel

Shallow whole genome was successfully performed in 59 samples, and the release of tumor DNA (i.e., tumor fraction, TF) was detectable in 25 (39.7%) patients, with a median TF of 5.95% (range 2,3 – 74%) (Suppl. Table

◀**Fig. 2**. Genetic alterations on HRR genes identified on plasma of PCa patients (**A**) Oncoprint of genetic alterations identified on plasma samples. Patients in which no mutations are found are omitted. Columns represent individual plasma samples and are sorted by tumor fraction. Each gene affected by alterations has been reported and sorted by frequency (indicated on the left). The different colors represent the different alterations and the black circle indicates VUS, as indicated in the figure legends. The bar plots at the top and right of the oncoprint indicate the count of events found respectively in each sample and in each gene. In the lower part of the oncoprint, the tumor fraction calculated by sWGS (TF), time point (TP) and disease status (DS) are reported for each sample. (**B**) Deletion on *TP53* detected by HRS gene panel and visualized by IGV. Gray bars are the sequencing reads aligned to *TP53*, while the connecting black lines indicate the presence of the deletion. (**C**) Multiexonic deletion in *BRCA1* genes, detected by HRS gene panel and visualized by report generated with Sophia Genetics DDM® software. Coverage is normalized by sample (separately for each gene) and by the target region (using the automatically selected reference samples), and CNV detection is performed using a hidden-Markov-model algorithm. Each dot represents the copy number estimated by the software for each exon of *BRCA1* (exon 1 to 24). Blue dots indicate exons with no copy number variation, while red dots indicate the presence of a deletion.

ID	GENE	exon	cDNA	protein	VAF %	TF	WBC VAF%	Estimated origin
0130	*BRCA1*	ex 2 - ex 13	Deletion	–	40.0*	0.43	WT	somatic
0257	*BRCA2*	20	c.8614G > T	p.(Glu2872*)	54.7	0.34	WT	somatic
0432	*CDK12*	2	c.1224_1233del	p.(Ala409Glnfs*24)	32.5	0.45	WT	somatic
	CDK12	1	c.703_712del	p.(Asp235Argfs*100)	19.7		WT	somatic
0402	*BRCA1*	10	c.850 C > T	p.(Gln284*)	48.1	0.03	NA	germline
0292	*CHEK2*	14	c.1556 C > T	p.(Thr519Met)	45.3	0.03	NA	germline
0411	*ATM*	30	c.4611 + 9_4611del	–	51.1	0.00	43.5	germline
	ATM	57	c.8269G > A	p.(Val2757Met)	1.8		3.9	somatic-CH#
	ATM	58	c.8520_8524del	p.(Leu2840Phefs*6)	1.0		0.2	somatic-CH#
	ATM	63	c.9038T > A	p.(Leu3013Gln)	4.1		2.4	somatic-CH#
0554	*PALB2*	5	c.2167_2168del	p.(Met723Valfs*21)	50.1	0.00	46.1	germline
0165	*BRIP1*	3	c.139 C > G	p.(Pro47Ala)	50.3	0.02	NA	germline
0486	*ATM*	47	c.6908del	p.(Lys2303Argfs*7)	6.5	0.15	WT	somatic
0214	*CDK12*	1	c.678_679delinsA	p.(Trp227Glyfs*111)	1.7	NA	WT	somatic

Table 2. Classification of pathogenic mutations found on HRR mutant patients. Estimation of allele origin of the alteration was based on TF detected on plasma. When necessary WBC test was performed to validate origin and improve variant interpretation (according to scheme reported in S. Figure 2). *VAF estimated from the calculated copy number of 1.6. # CH = clonal hematopoiesis, confirmed on WBC. NA = not assessed.

1). Higher TF was observed in patients with metastatic disease with respect to localized disease even if it did not reach significance (Suppl. Figure 1), conversely a significant association was found with prior RT ($\rho = 0.019$). To better explore the association between RT and ctDNA positivity, we performed further analyses by considering RT time (from RT to the plasma collection time) and RT approach (adjuvant, radical RT or treatment of patients with relapsed carcinoma), but no significant associations were found ($P = 0.162$ and $P = 0.209$, respectively). Other clinicopathological characteristics of patients (localized vs. metastatic) or sample time points (baseline vs. during treatment) did not significantly influence TF (Suppl. Table 3).

TF estimated in each sample allowed an improvement in the variant interpretation (Suppl. Figure 2). At first, sWGS allowed us to identify clear germline mutations from putative somatic events. In fact, a germline origin of high-VAF variants (> 40%) can be assumed if TF is low (< 10%). In support of this, target sequencing of the WBC counterpart confirmed the classification and a good correlation was found between the TF and the VAF of the remaining putative somatic variants ($R^2 = 0.69$) (Suppl. Figure 3). Lastly, the combination of sWGS allowed to identify samples 'non-informative' (46% of the samples in our cohort), in which the absence of mutations in target genes support a lack of germline HRR alterations, but the lack of detectable TF do not provide information about the somatic alterations (Suppl. Table 1, Suppl. Figure 4).

Considering only the "informative" plasma samples, a proper HRR status was defined for 30 patients of which 10 were classified as HRR mutated. Among these, 5 cases presented germline alterations, while two clonal haematopoiesis events involving the *ATM* gene were identified (Table 2).

Concordance agreement between plasma and matched FFPE tumor tissue

Among the PCa cohort analyzed, matched FFPE tumor tissue was available for 41 patients, and it was processed for analysis of both the HRS and sWGS. The HRS analysis was efficiently performed on almost all patients (39/41). Since more than one mutation were identified in several samples, the concordance between plasma and FFPE tissue was estimated both for the overall mutational status of the HRS panel ("HRS status") classification and for the specific mutations detected. The HRS status was concordant in 41% of the patients; however, if only

"informative" plasma samples were considered, the concordance rate increased to 78.9%. Interestingly, true-positive calls can still be detected among low VAF variants in samples with low TF, and through manual curation 3 additional concordant mutations were found at low VAF (0.6-0.8%), raising the concordance rate to 85.7%. Among the concordant samples, 67% were mutated, and 33% were WT for HRS genes in both plasma and tissue samples. This substantial agreement was also supported by the Kappa coefficient of 0.69 ($p < 0.001$) (95% CI: 0.36–1.01, $p < 0.001$) and a PABAK of 0.71 (95% CI: 0.27–0.94). Notably, among patients with "non-informative" plasma, 10 additional cases of HRS-altered PCa cases could be detected from FFPE tissue analysis only (Fig. 3A; Suppl. Table 1).

Concordance was then evaluated for each specific mutation. Considering only patients with "informative" plasma and matched FFPE tissue, 30 alterations in the HRS genes were detected: 15 (50%) were concordant, 10 (33.33%) were detected only in plasma, and 5 (16.67%) were detected only in FFPE (Fig. 3B).

Globally, the discordant mutations were detected at a lower VAF than the concordant mutations in the plasma samples (Fig. 3C). Interestingly, nearly half of the discordant alterations belonged to two plasma samples (patients 526 and 411). Evaluation on WBC counterpart of these discordant alterations disclosed a CH origin in 8 out of 10 variants (Suppl. Table 1). The remaining two alterations were detected at low VAF (1,6–2%) in a plasma sample with low TF, however deep sequencing of the locus in the WBC did not reveal these mutations, supporting a somatic origin of these variants (Suppl. Table 1).

Estimation of copy number variations from plasma

Exploratively, sWGS analysis was also used for the characterization of tumor CNV. In particular, sWGS and CNV analysis were successful for 31 FFPE samples (Suppl. Table 4). The CNV profile of the cohort is in accordance with the literature on PCa, with high frequency of CNV involving 8q amplification and 8p, 10q, 13q, 15q, 16q and 18q deletions (Fig. 4A).

Then, we assessed the feasibility of estimating CNV in plasma specimens, considering only samples with at least 3% TF. A total of 26 plasma samples were analyzed, and their CNV plasma profiles were similar to what was expected. Indeed, the CNV profile identified in plasma was consistent with the CNV profile identified in the corresponding FFPE tissue and was in line with what is commonly found in PCa datasets available online (Fig. 4A). A median of 13 (range 1–49) CNV per plasma sample were identified (Suppl. Table 5), corresponding to a median CNV burden of 26.53%. .

However, the ability of sWGS to identify CNV from plasma was affected by the quantity of TF in each sample. As preliminary data, the number of regions affected by CNV was compared in 10 matched plasma/FFPE patients (Fig. 4B). As a demonstration of that, the burden of CNV alterations in plasma samples, in terms of the number of events and the fraction of the genome altered, was positively associated with higher TF (Fig. 4C,D).

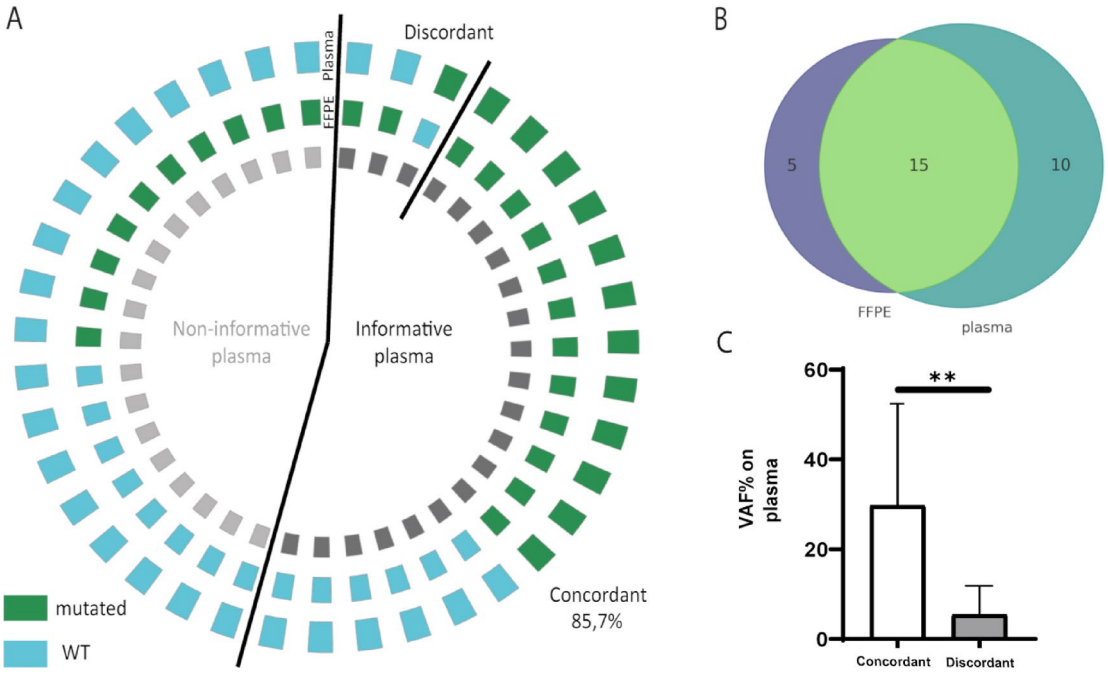

Fig. 3. Concordance of mutations on HRS genes identified in matched plasma and FFPE samples. Concordance of mutations on HRS genes identified in matched plasma and FFPE samples. (**A**) HRS status overview of 39 patients with matched molecular determination on plasma and FFPE, considering ultra-low VAF% among "informative" plasma samples. (**B**) VENN diagram of mutations identified in cases with matched FFPE tissue and "informative" plasma. (**C**) Distribution of the VAF of concordant and discordant mutations. ** test-t p-value < 0.01.

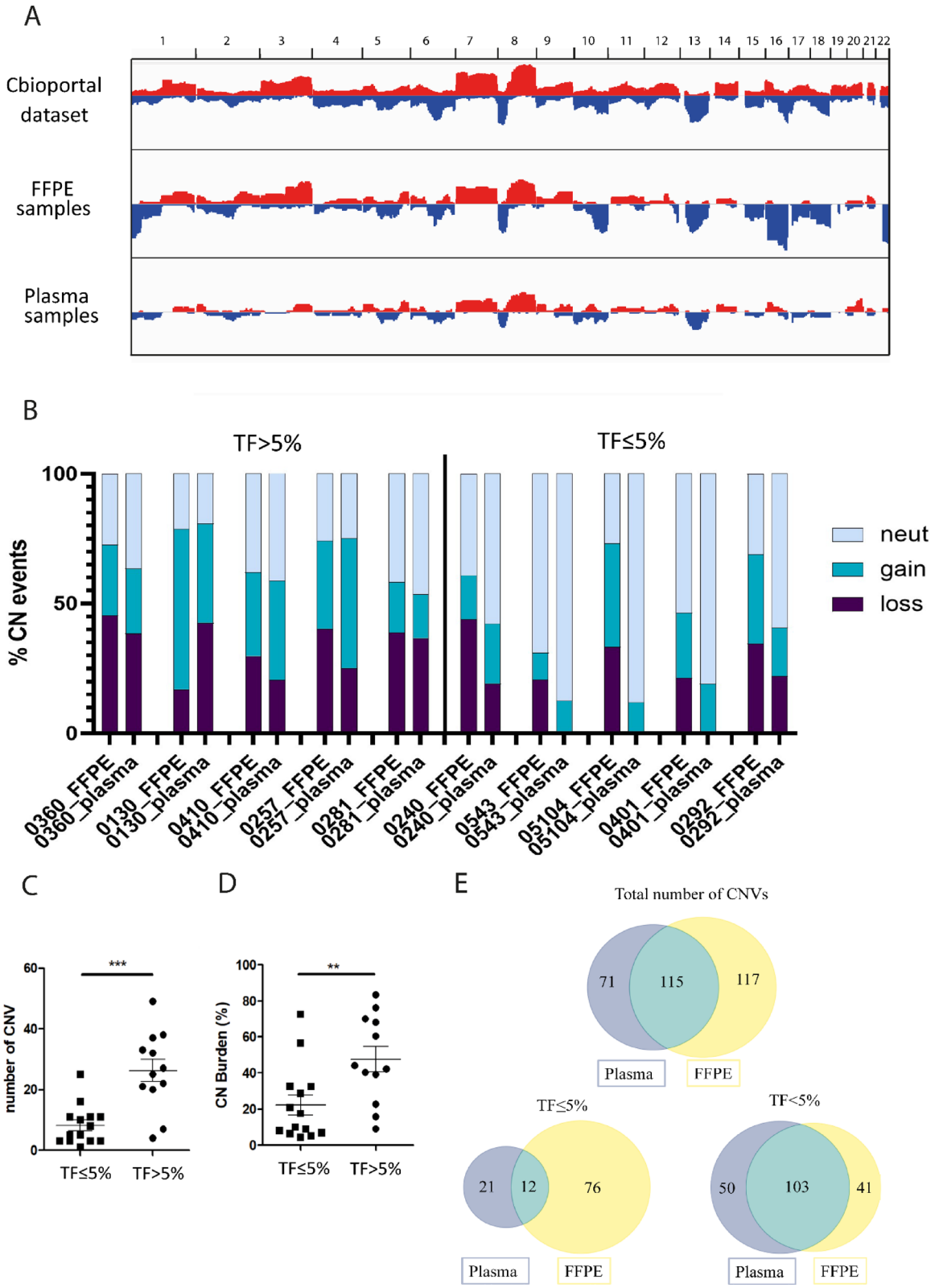

Fig. 4. Estimation of copy number variations from plasma sWGS analysis. (**A**) CNV trend distribution among autosomes in a public dataset of Cbioportal [Metastatic castration-sensitive prostate cancer (MSK, Clin Cancer Res 2020)][39]FFPE and plasma samples of our case series. (**B**) The histogram showed the percentage of genome altered by loss or gain CNV events in matched FFPE and plasma. Distribution of CNV among matched samples are described and ordered by TF (right of the line TF > 5%, left lower TF ≤ 5) (**C**) The number of CNV events and (**D**) the CN burden in TF ≤ 5% and TF > 5% plasma samples. (**E**) VENN plot of paired CNVs detected between plasma and FFPE tissue, total number of CNVs (top) and separated by TF > 5 or TF ≤ 5 (bottom). Abbreviations: CN, copy number, TF, tumor fraction.

A strong correlation was observed between CNVs identified in plasma with high TF (greater than 5%) and those identified in the corresponding FFPE samples, with 71.5% of CNVs detected in FFPE also being detectable in matched plasma. Conversely, a poor ability to detect real CNV was found in low releasing plasma (Fig. 4E).

Discussion

This study highlights the utility of liquid biopsy for molecular profiling in PCa, particularly in advanced stages where genomic insights are essential for guiding personalized therapies like PARPi. Traditional tissue biopsies face challenges such as tumor heterogeneity, poor archival sample quality, and the predominance of bone metastases, which limit high-quality DNA extraction[40,41]. Moreover, relapse commonly occurs several years after diagnosis[42,43]so surgical tissues are usually collected many years before systemic or targeted therapy needs to be decided. Liquid biopsy has emerged as a less invasive and more accessible alternative, with recent FDA approvals confirming its potential for clinical use[44]. Moreover, the handling and processing of liquid biopsy specimens is faster, reducing handling cost and time for analysis.

However, the concordance rate of variants between tissue and plasma remains a major concern in clinical practice[45]. In this study, we performed capture-based targeted sequencing using a panel consisting of 16 cancer HRR genes in plasma samples derived from 63 PCa patients. Through this approach we identified HRR mutations in 15.8% of patients, consistent with reported mutation frequencies in advanced PCa ranging from 11 to 33%, depending on the number of genes analyzed[46,47]. One of the limitations of NGS analysis on liquid biopsy analysis is the detection of large deletions and homozygous focal deletions[48]. Interestingly, in the present study, we identified novel pathogenic deletions in *TP53* and a large multiexonic deletion in *BRCA1* in plasma samples using the HRS target panel. This finding highlights the feasibility of employing such an approach to identify even complex alterations, however we cannot exclude that homozygous focal deletions can be missed by the assay[38].

Notably we combined the mutational analysis with the TF estimate obtained by sWGS. Despite release of tumor DNA being detectable in only 39.7% patients, the addition of this information produced an improvement of HRR mutational call, with the identification of non-informative plasma and the identification of germline events. In particular, up to 46% of samples in our cohort were classified as non-informative, indicating that the full somatic HRR status of these patients cannot be defined and that they will benefit for the addition of further testing in the somatic tissue or from plasma samples collected at later timepoints such as during an active phase of the disease or at relapse. Moreover, through TF estimates we were able to classify germline events, which affected half of our HRR mutant cases. The blood testing was then used for the validation of these findings and for the exclusion of CH. Considering the inactivation of HRR-associated genes, several authors have shown similar frequencies of somatic and germline mutations in different pathological stages of PCa. However, in many research studies, somatic and germline mutations are often grouped together without differentiation[11,48–50].

This study highlights the high frequency of non-informative plasma samples due to insufficient tumor DNA release, limiting HRR status assessment. Despite the mutational panel's high sensitivity, the sWGS pipeline used here has a LOD of 3% TF. Combining fragmentomics or methylation profiling[51,52] with an HRR-targeted panel could improve sensitivity and reduce non-informative cases.

For such samples, retesting with alternative biospecimens is necessary, such as FFPE tissue or, in the case of liquid biopsy, samples collected before therapy or at disease progression, as ctDNA levels may fluctuate during treatment. Approaches to enhance ctDNA release in plasma are under investigation, however external factors such recent meals, time of the day or physical activity before blood drawn do not seem to influence ctDNA release[53,54].

To evaluate the role of liquid biopsy in the HRR profiling of PCa patients, we compared our results on plasma with matched FFPE samples. The concordance rate of 85.7% between plasma and tissue analyses in informative samples aligns with literature-reported rates of 70–90%, validating the robustness of liquid biopsy for detecting actionable mutations[48,55,57]. In particular, we were able to identify 2 plasma alterations at very low VAFs (0.7% and 0.8%) that were present in the same matched FFPE samples. WBC negative analysis of the detected ultralow-VAF% alterations confirmed somatic origin, consistent with the high sensitivity of the target panel assay. Nevertheless, alterations in low-TF plasma (< 5%) require the characterization of matched WBCs or tumor tissue, if available, to exclude CH events or to confirm somatic origin, respectively[57,58].

In fact, we identified CH-related alterations affecting *ATM* and *TP53* in our cohort. In the present study, WBC analysis supported the determination of mutation origin—clonal hematopoiesis (CH), germline, or somatic—for mutations that were more difficult to interpret. However, WBC analysis was not available for all cases, and other CH events were excluded based on VAF and TF values. Other CH events CH refers to the presence of genetically distinct blood cells arising from a single hematopoietic stem cell, often associated with aging and certain genetic mutations[59]. In the context of PCa and particularly mCRPC, the detection of CH can complicate the interpretation of genetic testing results, especially when utilizing liquid biopsies to analyze ctDNA[60]. Thus, in case of low VAF variants affecting genes frequently involved by CH, tumor tissue and blood samples testing still remains the most suitable method to ensure accurate interpretation[61].

Finally, Genome-wide CNV analysis of plasma samples is still a challenge, as demonstrated by several studies[62–64]. In the present study, sWGS approach further enhanced profiling by reliably identifying copy number variations, with plasma CNV profiles correlating well with matched tissue samples and published PCa datasets[65]. However, our data also highlight the challenges posed by low ctDNA levels in certain plasma samples, which can limit detection sensitivity and necessitate complementary analysis methods.

Notably, CNV and SNP profiling via tumor-enriched liquid biopsy may spare invasive diagnostic investigations, such as tissue biopsy, and can be an excellent monitoring tool for unique blood-based testing methods[65]. The TF itself holds significant value in characterizing alterations and can serve as a standalone biomarker[66,67]. The low percentage of plasma samples with detectable TF is consistent with previous data reported in PCa, in which low and variable level of ctDNA is still a challenge. Fonseca et al., reported that 40% of PCa plasma

samples can have ctDNA fraction below 2%[68], and Jayaram et al. reported a detection rate between 19% and 50% depending on the time of plasma collection (pre-treatment, during treatment and at PD[69]. The heterogeneity of the cohort analyzed in this study limited the depth of statistical analysis between HRR status and clinical outcomes. However, a key strength of the methodology employed here is its ability to assess whether a sample provides meaningful information, irrespective of the time it was collected. In our study, TF was not significantly affected by the time of plasma collection (baseline, on treatment, or at the PD). Even if not significant, a trend toward high levels of ctDNA metastatic diseases and with high Gleason score was found. Moreover, a significant association between radiation therapy and ctDNA positivity in the samples. The data suggest the usefulness of ctDNA testing as an early detection biomarker after surgery and for disease monitoring during progression[70]. However, an association with clinical outcome was not performed due to the heterogeneity of the case series.

In conclusion, the combined mutational and sWGS approach presented in the present study can be a valuable tool for both patient selection in PARPi regimens and patient monitoring during PARPi treatment. Indeed, this assay identified both SNPs and CNVs, it was able to classify germline variants and to overcome the bias of false-negative results, identifying "non-informative" samples (i.e., plasma with no mutation and no TF) from real-negative patients (plasma with no alteration in ctDNA). Despite the retrospective design, small cohort, and nonsimultaneous collection of tissue and plasma samples, this study demonstrates the feasibility of ctDNA testing for comprehensive molecular characterization in PCa, especially when tissue samples are unavailable or inadequate. The results from the present study showed that mutational and CNV analysis performed on tumor-informed liquid biopsy samples are useful for the molecular characterization of prostate cancer and that liquid biopsy maintains a key role in the management of prostate cancer patients. Future prospective studies with larger cohorts are warranted to validate these findings and further explore the clinical utility of ctDNA-guided treatment strategies.

Data availability

The data that support the findings of this study are available in the supplementary material of this article, and additional data are available upon request to the corresponding author. No restrictions apply. The CNV profiles of public available prostate cancer datasets downloaded from cBioPortal [Metastatic castration-sensitive prostate cancer (MSK, Clin Cancer Res 2020) doi:10.1158/1078-0432.CCR-20-0168][40].

Received: 5 December 2024; Accepted: 2 June 2025
Published online: 01 July 2025

References

1. Rawla, P. Epidemiology of prostate cancer. *World J. Oncol.* **10** (2), 63–89. https://doi.org/10.14740/wjon1191 (2019).
2. Sung, H. et al. Global Cancer statistics 2020: GLOBOCAN estimates of incidence and mortality worldwide for 36 cancers in 185 countries. *CA Cancer J. Clin.* **71** (3), 209–249. https://doi.org/10.3322/caac.21660 (2021).
3. Siegel, R. L., Miller, K. D., Fuchs, H. E. & Jemal, A. Cancer statistics, 2022. *CA Cancer J. Clin.* **72** (1), 7–33. https://doi.org/10.3322/caac.21708 (2022).
4. Kodama, H. et al. Castration-resistant prostate cancer without metastasis at presentation May achieve cancer-specific survival in patients who underwent prior radical prostatectomy. *Int. Urol. Nephrol.* **52** (4), 671–679. https://doi.org/10.1007/s11255-019-02339-3 (2020).
5. Hamid, A. A. et al. Compound genomic alterations of TP53, PTEN, and RB1 tumor suppressors in localized and metastatic prostate cancer. *Eur. Urol.* **76** (1), 89–97. https://doi.org/10.1016/j.eururo.2018.11.045 (2019).
6. Conteduca, V., Brighi, N., Schepisi, G. & De Giorgi, U. Immunogenomic profiles associated with response to life-prolonging agents in prostate cancer. *Br. J. Cancer.* **129** (7), 1050–1060. https://doi.org/10.1038/s41416-023-02354-3 (2023).
7. Conteduca, V. et al. Plasma androgen receptor and docetaxel for metastatic Castration-resistant prostate Cancer. *Eur. Urol.* **75** (3), 368–373. https://doi.org/10.1016/j.eururo.2018.09.049 (2019).
8. Salvi, S. et al. Circulating AR copy number and outcome to enzalutamide in docetaxel-treated metastatic castration-resistant prostate cancer. *Oncotarget* **7** (25), 37839–37845. https://doi.org/10.18632/oncotarget.9341 (2016).
9. Gandhi, J. et al. The molecular biology of prostate cancer: Current Understanding and clinical implications. *Prostate Cancer Prostatic Dis.* **21** (1), 22–36. https://doi.org/10.1038/s41391-017-0023-8 (2018).
10. Chung, J. H. et al. Prospective comprehensive genomic profiling of primary and metastatic prostate tumors. *JCO Precis Oncol.* https://doi.org/10.1200/PO.18.00283 (2019).
11. de Bono, J. et al. Olaparib for metastatic Castration-Resistant prostate Cancer. *N Engl. J. Med.* **382** (22), 2091–2102. https://doi.org/10.1056/NEJMoa1911440 (2020).
12. Hussain, M. et al. Survival with Olaparib in metastatic Castration-Resistant prostate Cancer. *N Engl. J. Med.* **383** (24), 2345–2357. https://doi.org/10.1056/NEJMoa2022485 (2020).
13. Fizazi, K. et al. Rucaparib or physician's choice in metastatic prostate Cancer. *N Engl. J. Med.* **388** (8), 719–732. https://doi.org/10.1056/NEJMoa2214676 (2023).
14. Chi, K. N. et al. Niraparib plus abiraterone acetate with prednisone in patients with metastatic castration-resistant prostate cancer and homologous recombination repair gene alterations: second interim analysis of the randomized phase III MAGNITUDE trial. *Ann. Oncol. Off J. Eur. Soc. Med. Oncol.* **34** (9), 772–782. https://doi.org/10.1016/j.annonc.2023.06.009 (2023).
15. Saad, F. et al. Olaparib plus abiraterone versus placebo plus abiraterone in metastatic castration-resistant prostate cancer (PROpel): final prespecified overall survival results of a randomised, double-blind, phase 3 trial. *Lancet Oncol.* **24** (10), 1094–1108. https://doi.org/10.1016/S1470-2045(23)00382-0 (2023).
16. Fizazi, K. et al. First-line Talazoparib with enzalutamide in HRR-deficient metastatic castration-resistant prostate cancer: the phase 3 TALAPRO-2 trial. *Nat. Med.* **30** (1), 257–264. https://doi.org/10.1038/s41591-023-02704-x (2024).
17. Grasso, C. S. et al. The mutational landscape of lethal castration-resistant prostate cancer. *Nature* **487** (7406), 239–243. https://doi.org/10.1038/nature11125 (2012).
18. Pritchard, C. C. et al. Inherited DNA-Repair gene mutations in men with metastatic prostate Cancer. *N Engl. J. Med.* **375** (5), 443–453. https://doi.org/10.1056/NEJMoa1603144 (2016).
19. Casadei, C. et al. Inherited mutations in DNA damage repair genes in Italian men with metastatic prostate cancer: results from the Meet-URO 10 study. *Eur. Urol. Open. Sci.* **61**, 44–51. https://doi.org/10.1016/j.euros.2024.01.015 (2024).
20. Parker, C. et al. Prostate cancer: ESMO clinical practice guidelines for diagnosis, treatment and follow-up. *Ann. Oncol. Off J. Eur. Soc. Med. Oncol.* **31** (9), 1119–1134. https://doi.org/10.1016/j.annonc.2020.06.011 (2020).

21. Schostak, M. et al. Practical guidance on establishing a molecular testing pathway for alterations in homologous recombination repair genes in clinical practice for patients with metastatic prostate Cancer. *Eur. Urol. Oncol.* **7** (3), 344–354. https://doi.org/10.1016/j.euo.2023.08.004 (2024).
22. Schmid, S. et al. Activity of Platinum-Based chemotherapy in patients with advanced prostate Cancer with and without DNA repair gene aberrations. *JAMA Netw. Open.* **3** (10), e2021692. https://doi.org/10.1001/jamanetworkopen.2020.21692 (2020).
23. Paschalis, A. et al. Prostate-specific membrane antigen heterogeneity and DNA repair defects in prostate Cancer. *Eur. Urol.* **76** (4), 469–478. https://doi.org/10.1016/j.eururo.2019.06.030 (2019).
24. De Giorgi, U. et al. Circulating androgen receptor gene amplification and resistance to 177Lu-PSMA-617 in metastatic castration-resistant prostate cancer: results of a phase 2 trial. *Br. J. Cancer.* **125** (9), 1226–1232. https://doi.org/10.1038/s41416-021-01508-5 (2021).
25. Conteduca, V. et al. Clinical and molecular analysis of patients treated with prostate-specific membrane antigen (PSMA)-targeted radionuclide therapy. *J. Clin. Oncol.* **37** (7_suppl), 272–272. https://doi.org/10.1200/JCO.2019.37.7_suppl.272 (2019).
26. Takamatsu, S. et al. Utility of homologous recombination deficiency biomarkers across Cancer types. *JCO Precis Oncol.* **6**, e2200085. https://doi.org/10.1200/PO.22.00085 (2022).
27. Nientiedt, C. et al. High prevalence of DNA damage repair gene defects and TP53 alterations in men with treatment-naïve metastatic prostate cancer -Results from a prospective pilot study using a 37 gene panel. *Urol. Oncol.* **38** (7), 637. e17-637.e27 (2020).
28. Abida, W. et al. Prospective Genomic Profiling of Prostate Cancer Across Disease States Reveals Germline and Somatic Alterations That May Affect Clinical Decision Making. *JCO Precis Oncol.* https://doi.org/10.1200/PO.17.00029 (2017).
29. Hussain, M. et al. Tumor genomic testing for >4,000 men with metastatic Castration-resistant prostate Cancer in the phase III trial profound (Olaparib). *Clin. Cancer Res.* **28** (8), 1518–1530. https://doi.org/10.1158/1078-0432.CCR-21-3940 (2022).
30. Zhu, J. et al. Clinical utility of foundationone tissue molecular profiling in men with metastatic prostate cancer. *Urol. Oncol.* **37** (11), 813e. 1-813.e9 (2019).
31. Kim, D. S., Camacho, C. V. & Kraus, W. L. Alternate therapeutic pathways for PARP inhibitors and potential mechanisms of resistance. *Exp. Mol. Med.* **53** (1), 42–51. https://doi.org/10.1038/s12276-021-00557-3 (2021).
32. Wang, J. et al. Exosomal MicroRNAs as liquid biopsy biomarkers in prostate cancer. *Crit. Rev. Oncol. Hematol.* **145**, 102860. https://doi.org/10.1016/j.critrevonc.2019.102860 (2020).
33. Goodall, J. et al. Circulating cell-free DNA to guide prostate cancer treatment with PARP Inhibition. *Cancer Discov.* **7** (9), 1006–1017. https://doi.org/10.1158/2159-8290.CD-17-0261 (2017).
34. Lin, K. K. et al. BRCA reversion mutations in Circulating tumor DNA predict primary and acquired resistance to the PARP inhibitor Rucaparib in High-Grade ovarian carcinoma. *Cancer Discov.* **9** (2), 210–219. https://doi.org/10.1158/2159-8290.CD-18-0715 (2019).
35. Vidula, N. et al. Routine Plasma-Based genotyping to comprehensively detect germline, somatic, and reversion BRCA mutations among patients with advanced solid tumors. *Clin. Cancer Res.* **26** (11), 2546–2555. https://doi.org/10.1158/1078-0432.CCR-19-2933 (2020).
36. Karczewski, K. J. et al. The mutational constraint spectrum quantified from variation in 141,456 humans. *Nature* **581** (7809), 434–443. https://doi.org/10.1038/s41586-020-2308-7 (2020).
37. Richards, S. et al. Standards and guidelines for the interpretation of sequence variants: a joint consensus recommendation of the American college of medical genetics and genomics and the association for molecular pathology. *Genet. Med.* **17** (5), 405–424. https://doi.org/10.1038/gim.2015.30 (2015).
38. Adalsteinsson, V. A. et al. Scalable whole-exome sequencing of cell-free DNA reveals high concordance with metastatic tumors. *Nat. Commun.* **8** (1), 1324. https://doi.org/10.1038/s41467-017-00965-y (2017).
39. Stopsack, K. H. et al. Oncogenic genomic alterations, clinical phenotypes, and outcomes in metastatic Castration-Sensitive prostate Cancer. *Clin. Cancer Res.* **26** (13), 3230–3238. https://doi.org/10.1158/1078-0432.CCR-20-0168 (2020).
40. Borbiev, T., Kohaar, I. & Petrovics, G. Clinical biofluid assays for prostate Cancer. *Cancers (Basel).* https://doi.org/10.3390/cancers16010165 (2023).
41. Martignano, F. et al. GSTP1 methylation and protein expression in prostate cancer: diagnostic implications. *Dis. Markers.* **2016**, 4358292. https://doi.org/10.1155/2016/4358292 (2016).
42. Caroli, P. et al. 68Ga-PSMA PET/CT in patients with recurrent prostate cancer after radical treatment: prospective results in 314 patients. *Eur. J. Nucl. Med. Mol. Imaging.* **45** (12), 2035–2044. https://doi.org/10.1007/s00259-018-4067-3 (2018).
43. Freedland, S. J. et al. Prostate size and risk of high-grade, advanced prostate cancer and biochemical progression after radical prostatectomy: a search database study. *J. Clin. Oncol.* **23** (30), 7546–7554. https://doi.org/10.1200/JCO.2005.05.525 (2005).
44. FDA. NGS FoundationOne®Liquid CDx assays FDA approval.
45. Kleftogiannis, D. et al. Detection of genomic alterations in breast cancer with Circulating tumour DNA sequencing. *Sci. Rep.* **10** (1), 16774. https://doi.org/10.1038/s41598-020-72818-6 (2020).
46. ICGC/TCGA Pan-Cancer Analysis of Whole Genomes Consortium. Pan-cancer analysis of whole genomes. *Nature* **578** (7793), 82–93. https://doi.org/10.1038/s41586-020-1969-6 (2020).
47. Ghose, A., Moschetta, M., Pappas-Gogos, G., Sheriff, M. & Boussios, S. Genetic aberrations of DNA repair pathways in prostate cancer: translation to the clinic. *Int. J. Mol. Sci.* https://doi.org/10.3390/ijms22189783 (2021).
48. Tukachinsky, H. et al. Genomic analysis of Circulating tumor DNA in 3,334 patients with advanced prostate Cancer identifies targetable BRCA alterations and AR resistance mechanisms. *Clin. Cancer Res.* **27** (11), 3094–3105. https://doi.org/10.1158/1078-0432.CCR-20-4805 (2021).
49. Lang, S. H. et al. A systematic review of the prevalence of DNA damage response gene mutations in prostate cancer. *Int. J. Oncol.* **55** (3), 597–616. https://doi.org/10.3892/ijo.2019.4842 (2019).
50. Teroerde, M. et al. Revisiting the role of p53 in prostate Cancer. In: (eds Bott, S. R. J. & Ng, K. L.) Prostate Cancer [Internet]. Brisbane (AU): Exon; (2021). May 27. Chapter 8.
51. Wong, D. et al. Early Cancer detection in Li-Fraumeni syndrome with Cell-Free DNA. *Cancer Discov.* **14** (1), 104–119. https://doi.org/10.1158/2159-8290.CD-23-0456 (2024).
52. Liu, Y. At the dawn: cell-free DNA fragmentomics and gene regulation. *Br. J. Cancer.* **126** (3), 379–390. https://doi.org/10.1038/s41416-021-01635-z (2022).
53. Kuligina, E. S. et al. Content of circulating tumor DNA depends on the tumor type and the dynamics of tumor size, but is not influenced significantly by physical exercise, time of the day or recent meal. *Cancer Genet.* **256–257**, 165–178. https://doi.org/10.1016/j.cancergen.2021.05.014 (2021).
54. Brown, J. C. et al. Effects of exercise on inflammation, Circulating tumor cells, and Circulating tumor DNA in colorectal cancer. *J. Sport Health Sci.* **17**:101036. https://doi.org/10.1016/j.jshs.2025.101036 (2025).
55. McFarland, T. R. et al. Detection of BRCA1, and BRCA2 alterations in matched tumor tissue and circulating cell-free DNA in patients with prostate Cancer in a real-world setting. *Biomedicines.* https://doi.org/10.3390/biomedicines10123170 (2022).
56. Lee, J. K. et al. The Pan-Tumor landscape of targetable kinase fusions in Circulating tumor DNA. *Clin. Cancer Res.* **28** (4), 728–737. https://doi.org/10.1158/1078-0432.CCR-21-2136 (2022).
57. Jensen, K. et al. Association of clonal hematopoiesis in DNA repair genes with prostate Cancer plasma Cell-free DNA testing interference. *JAMA Oncol.* **7** (1), 107. https://doi.org/10.1001/jamaoncol.2020.5161 (2021).

58. Aldea, M. et al. Liquid biopsies for circulating tumor DNA detection May reveal occult hematologic malignancies in patients with solid tumors. *JCO Precis Oncol.* **7**, e2200583. https://doi.org/10.1200/PO.22.00583 (2023).
59. Jaiswal, S. et al. Age-related clonal hematopoiesis associated with adverse outcomes. *N Engl. J. Med.* **371** (26), 2488–2498. https://doi.org/10.1056/NEJMoa1408617 (2014).
60. Severson, E. A. et al. Detection of clonal hematopoiesis of indeterminate potential in clinical sequencing of solid tumor specimens. *Blood* **131** (22), 2501–2505. https://doi.org/10.1182/blood-2018-03-840629 (2018).
61. Heitzer, E., Ulz, P. & Geigl, J. B. Circulating tumor DNA as a liquid biopsy for cancer. *Clin. Chem.* **61** (1), 112–123. https://doi.org/10.1373/clinchem.2014.222679 (2015).
62. Chae, Y. K. et al. Concordance of genomic alterations by Next-Generation sequencing in tumor tissue versus Circulating tumor DNA in breast Cancer. *Mol. Cancer Ther.* **16** (7), 1412–1420. https://doi.org/10.1158/1535-7163.MCT-17-0061 (2017).
63. He, Y. et al. Concordance of genomic profiles in matched tissue and plasma samples from Chinese patients with lung Cancer. *Clin. Med. Insights Oncol.* **16**, 11795549221116834. https://doi.org/10.1177/11795549221116834 (2022).
64. Wyatt, A. W. et al. Concordance of circulating tumor DNA and matched metastatic tissue biopsy in prostate Cancer. *J. Natl. Cancer Inst.*. https://doi.org/10.1093/jnci/djx118 (2017).
65. Grist, E. et al. Accumulation of copy number alterations and clinical progression across advanced prostate cancer. *Genome Med.* **14** (1), 102. https://doi.org/10.1186/s13073-022-01080-4 (2022).
66. Sophie, C. et al. A Tumor fraction to improve patient selection for oncology early phase clinical trials: Analysis of two precision medicine studies. In:; 2023:3005. (2023).
67. Choudhury, A. D. et al. Tumor fraction in cell-free DNA as a biomarker in prostate cancer. *JCI Insight*. https://doi.org/10.1172/jci.insight.122109 (2018).
68. Fonseca, N. M. et al. Prediction of plasma ctdna fraction and prognostic implications of liquid biopsy in advanced prostate cancer. *Nat. Commun.* **15** (1), 1828. https://doi.org/10.1038/s41467-024-45475-w (2024).
69. Jayaram, A. et al. Plasma tumor gene conversions after one cycle abiraterone acetate for metastatic castration-resistant prostate cancer: a biomarker analysis of a multicenter international trial. *Ann. Oncol. Off J. Eur. Soc. Med. Oncol.* **32** (6), 726–735. https://doi.org/10.1016/j.annonc.2021.03.196 (2021).
70. He, W., Xiao, Y., Yan, S., Zhu, Y. & Ren, S. Cell-free DNA in the management of prostate cancer: Current status and future prospective. *Asian J. Urol.* **10**(3), 298–316. https://doi.org/10.1016/j.ajur.2022.11.002 (2023).

Acknowledgements

This work was partly supported thanks to the contribution of Ricerca Corrente by the Italian Ministry of Health within the research line "Precision, gender and ethnicity-based medicine and geroscience: genetic-molecular mechanisms in the development, characterization and treatment of tumors.

Author contributions

V.C., U.D.G., P.U., A.V. and M.U. provided direction and guidance on the whole project. A.V., M.U, U.D.G., and P.U. drafted the manuscript. V.C., C.C., M.C.C., G.G., A.V., A.A.S., and G.D.L. carried out patient selection and sample collection. I.C., V.Z, A.V. and M.U. performed the laboratory experiments. M.U., P.U., A.V., G.T., and M.P. analyzed the data. M.P., D.A., and E.P. participated and performed the bioinformatics and statistical analysis. G.G., G.M., G.D.L., A.A.S., G.C., and U.D.G., reviewed the manuscript and made significant revisions. All authors reviewed and approved the final manuscript.

Funding

Not applicable.

Declarations

Competing interests

The authors declare no competing interests.

Ethical approval and consent to participate

All methods used in our studies involving human participants adhered strictly to the ethical guidelines of our institutional research committee, aligning with the principles outlined in the 1964 Helsinki declaration and its subsequent modifications, or equivalent ethical norms. This prospective study, with protocol code 0004169/2017 approved on 15/06/2017, was authorized by the Institutional Review Board of IRCCS Istituto Romagnolo per lo Studio dei Tumori (IRST) "Dino Amadori," Meldola, Italy.

Consent for publication

Not applicable.

Additional information

Supplementary Information The online version contains supplementary material available at https://doi.org/10.1038/s41598-025-05384-4.

Correspondence and requests for materials should be addressed to M.U.